BRNO UNIVERSITY OF TECHNOLOGY

VYSOKÉ UČENÍ TECHNICKÉ V BRNĚ

FACULTY OF MECHANICAL ENGINEERING

FAKULTA STROJNÍHO INŽENÝRSTVÍ

ÚSTAV VÝROBNÍCH STROJŮ, SYSTÉMŮ A ROBOTIKY

INSTITUTE OF PRODUCTION MACHINES, SYSTEMS AND ROBOTICS

EFFECTS OF NON-LINEAR STIFFNESS ON TURN PROCESS STABILITY IN HORIZONTAL TURNING MACHINES

VLIV NELINEÁRNÍ TUHOSTI NA STABILITU ŘEZNÉHO PROCESU U STROJŮ S VODOROVNOU OSOU SOUSTRUŽENÍ

PHD THESIS REPORT

TEZE DIZERTAČNÍ PRÁCE

AUTHOR
AUTOR PRÁCE

Ing. PETR HADRABA

SUPERVISOR
VEDOUCÍ PRÁCE

doc. Ing. ZDENĚK HADAŠ, Ph.D.

BRNO 2023

Keywords

Chatter, Nonlinear dynamics, Linear ball guideway, Lathe

Klíčová slova

Samobuzené vibrace při obrábění, Nelineární dynamika , Lineární kuličkové vedení, Soustruh

Contents

1 Introduction **5**

2 Aims of PhD. Thesis **6**

3 Chatter – Self-exited Vibration in Machining Process **6**
3.1 Chatter stability estimation in turning process 7
3.2 Current research in the field of self-excited vibrations 8

4 Problem of Unpredictable Vibration During Machining Process **9**

5 Simplified 2D Analysis and Linearisin at Opperating Point Synthesis Algorithm **10**
5.1 Linear Model 11
5.2 Proposed Synthesis of Linearization in Operating Points Algorithm for Chatter Analysis of Structure With Nonlinear Stiffness 13
5.3 Dynamic Response of Simulated Modal Hammer Impulse and Comparison of SLOP Lobe Diagram With Time-domain Simulation 14

6 Nonlinear Analysis Using Substructuring Approach **16**
6.1 Reaction in linear ball guideway analysed by multibody based s on static load reaction analysis 18
6.2 Frequency Responses and Impact Simulation 19

7 Chatter Stability and Frequency Estimation Application of SLOP Algorithm **20**

8 Experimental Setup **22**
8.1 Comparison of Simulated Impulse with Impulse Hammer Measurements . 22
8.2 Experimental Machining Trials for Chatter Behaviour Verification 23

9 Results and Discussion **24**

10 Proposed Methodology of Machine-Tool Design **26**

11 Summary of Work Benefits **28**

12 Conclusion **29**

1 Introduction

The machine tool industry is facing productivity saturation and lags behind other fast-developing industrial fields. The reason is that the investment horizon of new machine tools is quite long. It is not unusual to see working machines built several decades ago. Moreover, traditional cam-based machine tools could even exceed the productivity of modern CNC machines. Therefore, there is not much space for new progressive development. Despite this fact, there is a significant obstacle in the machining industry, the lack of skilled machinists, which brings a new challenge in this century, how to decrease the number of human labour needs in machining. Industry 4.0 should be an answer to this issue. Digitalisation and the Internet of Things should optimise the workflow in factories and enable production with minimal needs for human workers. In contrast to a problem with a self-driving car, machine tools work in a controlled manner. However, the machine man still needs long-term experience and good knowledge of the machine for the best results. One of the signs of mastering machine tools is to use maximal productivity of the cutting process without vibration. Without a well-defined limit of chatter stability, it is impossible to achieve high productivity without an experienced operator.

The chatter phenomenon is familiar to anyone who operates machine tools. Most operators can easily recognise an unstable cut by sound during machining and the quality of the workpiece surface. Although chatter theory has been well known for a long time, many types of uncertainty complicate its application. Most processes are based on machinist senses and experience rather than chatter analysis.

Many parameters cause uncertainties: the inconsistency of the workpiece's material property, knife wear, changeable behaviour of the machine tool dynamic due to its dependence on tool position, machining parameters dependency of specific cutting force on the machining conditions, changeable behaviour of the machine's dynamic which dependence on tool position, the process damping during machining or nonlinearities of the structure – all these factors influence the stability of machining. All these factors limit the use of a simple lobe diagram to a specific case. However, with the decreasing number of highly skilled workers who could adjust the process based on their experience and the increasing effort to replace human labour, the importance of reliable stability prediction increases significantly.

This thesis tries to find an answer to one of these aspects which complicates the reliability of the stability diagram, the effect of nonlinear stiffness on the machine tool stability. The motivation for this work was the author's experience with stability prediction, which often differs from measured experimental machining. The most suspicious was the frequency shift of the excited chatter vibration, where a change in stiffness must be the cause. Therefore, it is necessary to find methods to predict this kind of behaviour.

2 Aims of PhD. Thesis

Although nonlinearities are a natural part of machines, they are caused by many different: structural, contact, or otherwise causes; they are often not considered in the design and operation of machines. This work aims at a description of stability prediction and defines a methodology for chatter stability prediction, which could enable better machine tool design and improve the targeting of active chatter suppression.

- Analysis of the influence of nonlinearity of bonds on the stability of the cutting process
- Methodology for the construction of machine tools in terms of increasing stability of self-excited vibrations
- Analysis of the possibilities of nonstructural increase of cutting stability of machine tools

3 Chatter – Self-exited Vibration in Machining Process

In the theory of self-excited oscillations, there are two basic models describing stability during machining:

- Mode coupling effect
- Regenerative chatter.

Tlusty describes the principle of positional coupling, which enables to describe some of the occurrence of vibrations during machining of a material that is not corrugated from the previous operation (e.g., linear planing) [1]. The model is based on a system with two different perpendicular stiffness. Therefore, the basis is an oscillation model with two

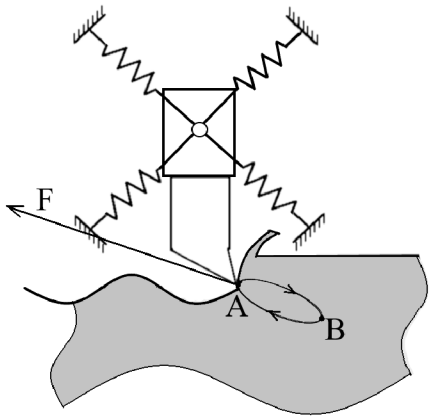

Figure 1: Mode coupling effect scheme

degrees of freedom and a different natural frequency for each direction. The tool performs an elliptical movement during machining. If we consider the system from Fig. 1 and the movement in a clockwise direction, when moving from A to B, the width of the depth of cut decreases, so the force is less than when cutting from B to A. Assuming that the

energy supplied in this way is greater than the energy wasted by damping, the system increases its oscillation.

The regenerative chatter principle is based on the interaction between surfaces that happen in the previous turn and the actual blade deflection of the knife. Fig. 2 shows a simplified model with an example of the dependence of the stability on the phase shift between the actual and previous cut. A stable cut occurs when the phase shift is small, the cutting force is therefore almost constant even during the initial undulation of the surface; the cut will gradually calm down in this case, as this system will not be supplied with new energy. The opposite case occurs when the phase shifts pi then the minimum and maximum cuts alternate, which excites the system with a variable cutting force.

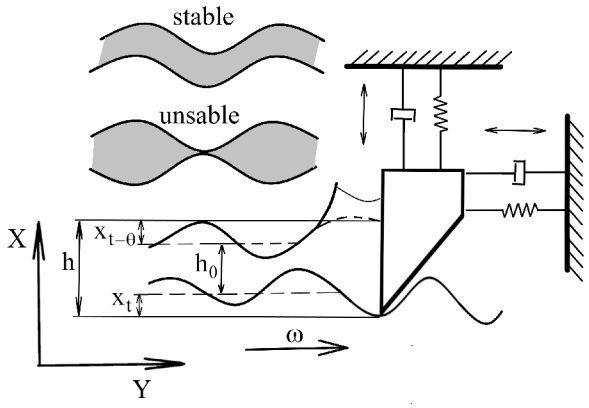

Figure 2: Regenerative chatter scheme

Both of these models require a range of simplifying assumptions, such as the independence of the cutting resistance from the depth of the cut, a constant angle of the cutting force vector to the surface, etc. All these simplifications are essential in most cases, but there are cases where neglect of some effects is very significant.

3.1 Chatter stability estimation in turning process

The key is to define conditions when the system will be stable and unstable, Tlusty defined it by a limit width of the chip b_{lim} as a fraction where cutting force Ks and negative real part of system's transfer function $G(u)$ are in the denominator:

$$b_{lim} = \frac{-1}{2K_s G(u)}. \tag{1}$$

If we consider a minimum of negative real functions $min(G(u))$ then we get the criteria for the whole spindle speed stability. However, this criterion is too strict, so the next step in classical analysis is to define the faze shift ϵ, which is the inverse tangent of the fraction of the real and imaginary part of the transfer function:

$$\epsilon = atan\left(\frac{real(G(u))}{imagG(u)}\right). \tag{2}$$

The last step before building up the lobe diagram is to calculate the reaction frequency f_{r_i} for each harmonic lobe.

$$f_{r_i} = \frac{f_s}{i - \frac{\epsilon}{\pi}}; \quad i = 1, 2, 3...n. \tag{3}$$

Combining the reaction frequency width criterion to limit the stable chip width, we get a stability lobe diagram; this diagram draws the boundary between stable and unusable conditions, the typical diagram can be seen in Fig. 3 [1, 2].

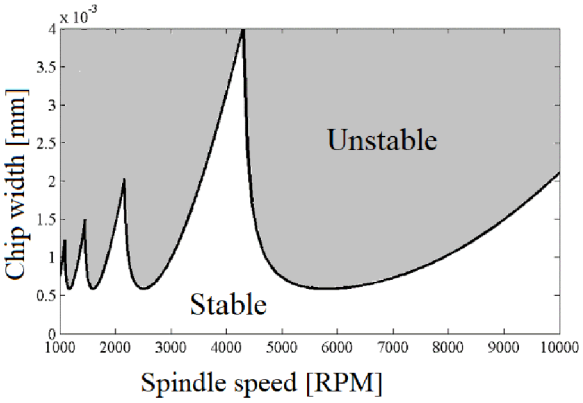

Figure 3: Lobe diagram divides machining condition on stabile and unstable

3.2 Current research in the field of self-excited vibrations

Today's trend is, above all, a better description of the machining process and the connection of individual influences on the stability of the cutting process. These are the parameters of the cutting process, where the friction between the tool back and the chip, the shear stress in the chip and the angle of inclination of the cutting edge affect the direction of the force result. It should be noted that these properties are also related to chip temperature.

Jiang focuses on experimental verification of lathe stability estimation, which assumes a flexible workpiece and considers nonlinear cutting resistance [3], its proposed model compares with the results using the method presented by Altintas [4]. Altintas addresses, among other things, the difference between numerical simulation and analytical solution. Where Altintas addresses, among other things, the difference between numerical simulation and analytical solution. Furthermore, this work deals with the FEM simulation of the cutting process. Ayed using FEM compares the properties of cutting parameters depending on the grain structure of the titanium alloy [5].

Most works assume cutting resistance coefficients obtained from measurements of a stable machining process. Turkes uses a piezo actuator-driven cutting process to obtain dynamic cutting forces and, at the same time, focuses on the effect of material damping on machining stability[6]. Several works deal with process damping. Due to process damping at a low spindle speed, the machine stability increases significantly. However, the process damping depends on a large number of parameters, especially on the degree of cutting edge wear, so its estimation is not a simple task. Due to the complexity of this problem, many works are devoted to it, e.g. [7, 8, 9].

One part of the research direction of self-excited vibrations focuses on thin-walled components machining when the rigidity of the workpiece significantly influence the overall stability of the system. Rubeo deals with this issue and presents time simulations, which he validates by measurement [10].

4 Problem of Unpredictable Vibration During Machining Process

Unexpected vibrations occur with the newly developed multi-spindle lathe support(see Fig. 4). In the part of the speed spectrum, the machine behaves following the theory of regenerative self-excited vibrations during machining.

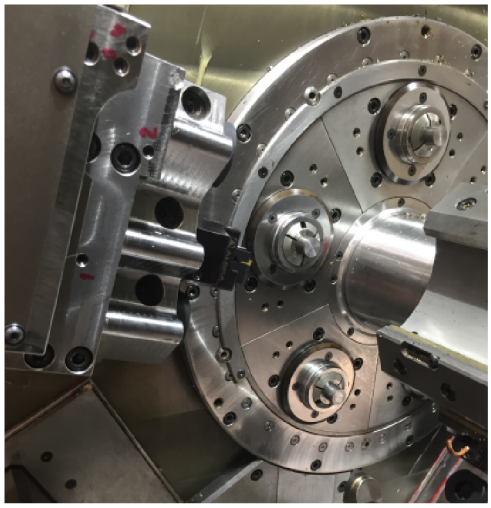

Figure 4: Measured dynamic compliance of the new slide

Figure 5 measured dynamic compliance in three directions XYZ as a response to hammer hit in these directions. It shows that the highest amplitudes are in the first mode approximately on 48 Hz; this mode is dominant in the plane Y-Z. The second mode (71 Hz) is dominant in the X direction with the second-highest amplitudes, with the increasing frequency amplitudes hights decrease rapidly.

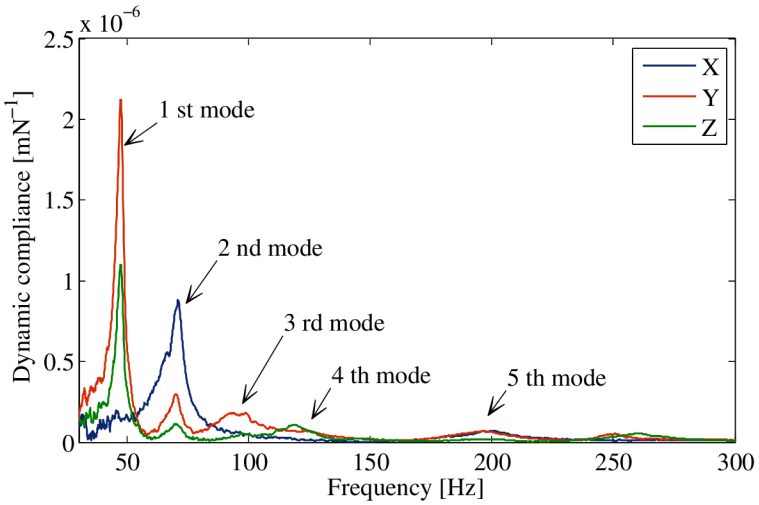

Figure 5: Measured dynamic compliance of the new slide

Using standard chatter theory (described in the previous chapter) can easily create a lobe diagram and a chatter frequency diagram Fig. 6. These two figures show an apparent match between frequency measurement and the prediction for spindle speed

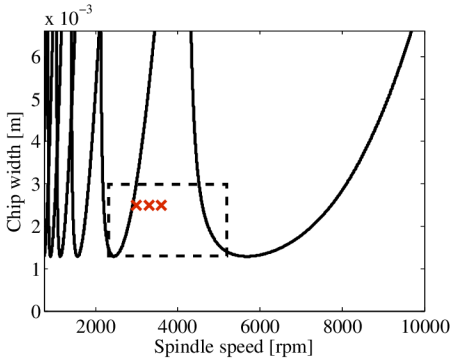

(a) Full scale diagram

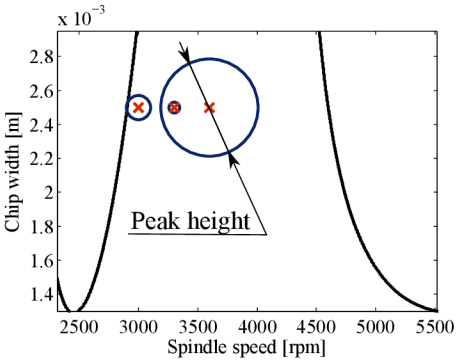

(b) Detail with signal strength representations

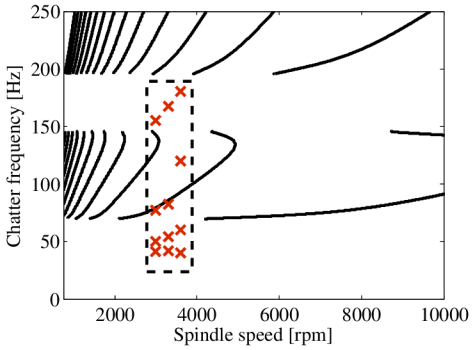

(c) Full scale diagram

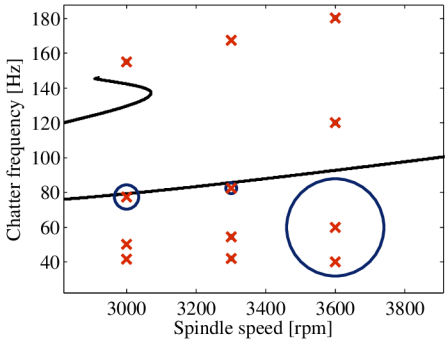

(d) Detail with signal strength representations

Figure 6: Predicted lobe diagram compared with measured machining conditions

3000 and 3300 rpm; despite stable cut prediction, the measurement follows the predicted trend where higher spindle speed increases stability. The inaccurate position of the lobe can be explained by the change in the specific cutting force.

In contrast, at 3600 rpm unpredicted behaviour is appeared, which has no basis in the chatter theory; in the theoretically stable condition, destructive chatter accrues, with the lower frequency that is for the chatter dominant second mode. Based on the frequency shift between the spindle speed and the excited chatter frequency, it can be concluded that the frequency of the natural frequency, which is the cause of the vibration, should be in the band around 54 Hz, which, however, has no support in the measurement.This fact leads to the hypothesis that the system's frequency response has to change. To rule out that the cause is the first mode of vibration that is closest. Therefore, the effect of the first mode must be ruled out.

5 Simplified 2D Analysis and Linearisin at Opperating Point Synthesis Algorithm

The simulation model is inspired by an engineering problem – tool damage caused by regenerative chatter in a theoretically stable area. The stability was estimated by an FEM (finite element model), a modal hammer measurement, and the experimental machining validated estimation. The result shows a good match in unstable regions; the chatter

frequencies match the predicted ones. However, the chatter arised in the theoretically stable region and its frequency do not correspond to the chatter frequency with a higher chip width. This behaviour leads to the hypothesis that it is the consequence of contact nonlinearity.

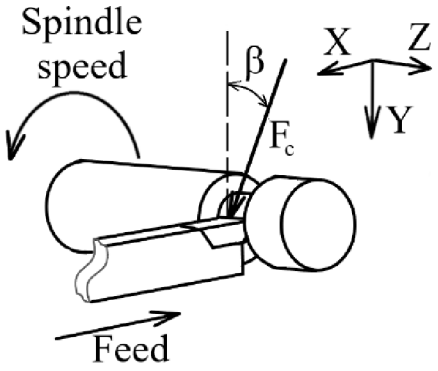

Figure 7: Grooving scheme

The analysis was done on the example of a grooving operation. Fig. 7 shows a scheme of the grooving process with the cutting force orientation; the cutting force lies in the plain XY where also lies the feed direction, which is oriented in the X direction. Due to this operation, the structure could be simplified as a two-dimensional problem, a beam with a two-spring support. This model describes mainly the first mode responsible for the chatter. However, the model has freedom in the Y direction; we consider movement only in the X direction and rotation in the Z axis. The scheme of the model could be seen in Fig. 8. The model is a rigid body represented by its mass and momentum of inertia in the center of gravity. This part connects the basis by two springs and dampers. In this case, the influence of the machine part stiffness is marginal, comparing the contact stiffness, so it is neglected.

5.1 Linear Model

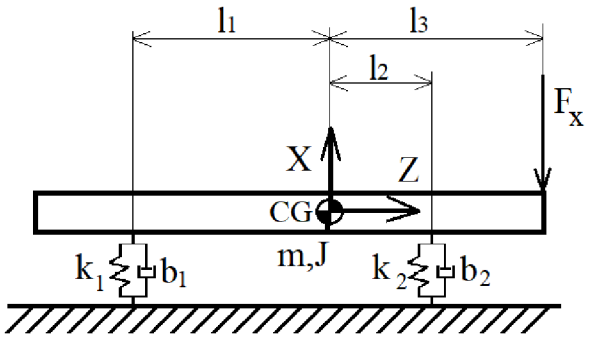

Figure 8: Scheme of parallel spring system

Regarding the previous assumptions, the model is represented by its momentum of inertia by two differential equations. The first represents the centre of gravity's displacement in the X-direction, and the second describes its rotation displacement.

$$m\ddot{x}, = k_1(x - l_1\theta) - k_2(x - l_2\theta) - b_1(\dot{x} + l_1\dot{\theta}) - b_2(\dot{x} + l_2\dot{\theta}) + F \tag{4}$$

$$J\ddot{\theta}, = k_1(x - l_1\theta)l_1 - k_2(x - l_2\theta)l_2 - b_1(\dot{x} + l_1\dot{\theta})l_1 - b_2(\dot{x} + l_2\dot{\theta})l_2 + Fl_3 \tag{5}$$

By transforming equations 4 and 5 to the matrix form, we get metrics **M**, **K**, **B**, and force vector **F**:

$$\mathbf{M} = \begin{bmatrix} m & 0 \\ 0 & J \end{bmatrix} \tag{6}$$

$$\mathbf{K} = \begin{bmatrix} k_1 - k_2 & -k_1 l_1 + k_2 l_2 \\ -k_1 l_1 + k_2 l_2 & -k_1 l_1^2 + k_2 l_2^2 \end{bmatrix} \tag{7}$$

$$\mathbf{B} = \begin{bmatrix} b_1 - b_2 & -b_1 l_1 + b_2 l_2 \\ -b_1 l_1 + b_2 l_2 & -b_1 l_1^2 + b_2 l_2^2 \end{bmatrix} \tag{8}$$

$$\mathbf{F} = \begin{pmatrix} 1 \\ l_3 \end{pmatrix} \tag{9}$$

Equation 10 provides the solution to the deflection and rotation in the centre of gravity x_{CG}, which depends on the angular speed of the harmonic force vector:

$$x_{CG}(\omega) = (\mathbf{K} - \omega^2\mathbf{M} + i\omega\mathbf{B})^{-1}F. \tag{10}$$

For a stability analysis, it is necessary to obtain a solution under the force. The total deflection is a combination of rotation and translation of the centre of gravity:

$$x_F(\omega) = (1, l_3)x_{CG}(\omega). \tag{11}$$

The damping values b_1, b_2 are represented by a simple linear model. The value of the damping coefficient was chosen to reach approximately 3 % of the critical damping of both modes for the linear structure. However, due to the nonlinear stiffness, the proportion of damping is changing. Due to the combination of preload and nonlinear stiffness, the nonlinearity of the whole linear ball guideway system is relatively high and causes changes in chatter stability. The behaviour can be easily described by the Hertzian contact between a ball and a groove contact. The simplest model is usually represented by a two-ball groove contact with a preload. Sun and Kong present this kind of model and use experimental validation to prove its behaviour [11], [12]. In the following work, Kong extends and presents a polynomial approximation of the linear ball guideway stiffness [13]. These more advanced models also consider the angular relations in the linear ball guideway. However, these models are too complicated and the primary behaviour matches the simple Hertzian contact model. The equation describes the basic Hertz contact model of the linear ball guideway stiffness:

$$F(x) = \begin{cases} k \cdot ((x_0 + x)^{3/2} - (x_0 - x)^{3/2}) & \mid x \mid < x_0 \\ k \cdot (x_0 + x)^{3/2} & x > x_0 \\ -k \cdot (x - x_0)^{3/2} & x < -x_0. \end{cases} \tag{12}$$

Where F is the reaction force of the contact, x_0 is the displacement caused by preload, k is the stiffness coefficient and x is a deflection from the equilibrium position of the guideway. The stiffness changes dramatically around the limit of the preload loss. If we consider that the loss of preload occurs when one row of the ball-groove contact has a

double preload deflection and the other is without any deflection, then we can define the contact loss load F_l as the proportion of the preload force F_p:

$$F_p = k \cdot x_0^{3/2}, \tag{13}$$

$$F_l = F_p \cdot \frac{(2x_0)^{3/2}}{x_0^{3/2}} = F_p \cdot 2^{3/2}. \tag{14}$$

Manufacturers usually declare that a lost preload load is $2.8 \cdot F_p$. The parameters are the preload force $F_p = 140\,N$ and the nonlinear stiffness coefficient $k = 7.55e9N/m^{3/2}$. For these conditions, we get the resulting dependence of stiffness on deflection in Fig. 9, where there is a noticeable region with stiffness decreasing by 30 %.

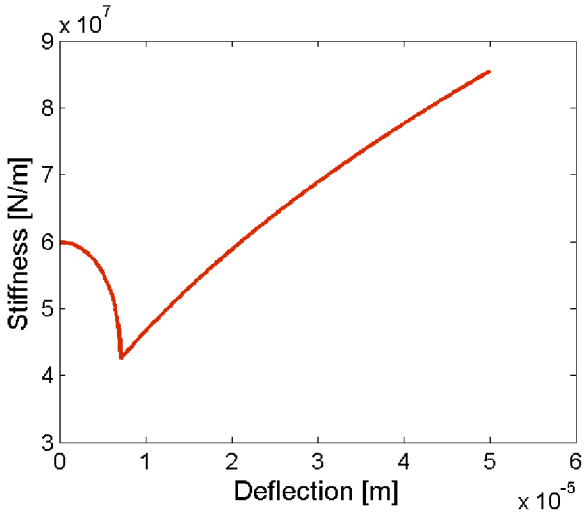

Figure 9: Stiffness dependency of models on the deflection

5.2 Proposed Synthesis of Linearization in Operating Points Algorithm for Chatter Analysis of Structure With Nonlinear Stiffness

The main idea of the synthesis of linearization in operating points algorithm (SLOP) is that the nonlinear structure under different loads has a unique set of linearized stiffness. Hence, it would also have a different stability lobe diagram (stability lobe diagram).

Fig. 10 shows the case of three different loads corresponding to different chip widths (each stability lobe diagram is valid only for a specific chip

width) the figure shows these areas as blue-stable and gray-unstable stripes. The final stability lobe diagram is composed of many of these local solutions; the total number depends on the required accuracy and the stability lobe diagram range. The assumption for the local linearization synthesis is that the chatter starts from a smooth surface with no other interruptions. According to this, the start of instability depends on the local behavior of the system. This is the reason why we can split the task of the lobe diagram into several subanalyses, and then the results of the local stability prediction are combined into one lobe diagram.

This algorithm aims at a fast detection of possible instability in the structure with height structural stiffness nonlinearity. The principle is to decompose the stability assumption problem into several subproblems. The first step is to define a range of stability

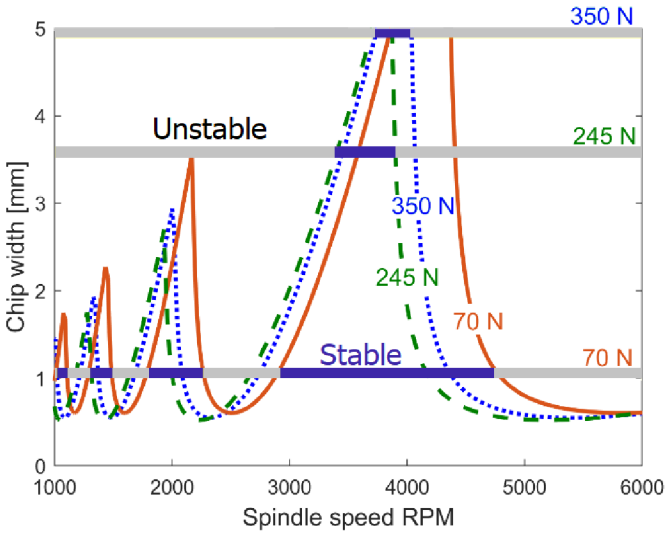

Figure 10: An example of the operation of an SLOP: three linearized stability lobe diagrams for different load segments corresponding to the chip width form the final stability lobe diagram

analysis and evaluate the cutting force applied during the stable machining process. After that, the nonlinear static analyses are applied to each of these loads. This analysis's required outputs are the stiffnesses of each connector, which is a linearization of each of these solutions. Before evaluating the system's general stability, the unstable solutions are excluded due to their transient behavior. Then, the unique sets of linearized stiffness combinations are used to create matrix K (equation 7) and compute a linear solution following equations 10 and 12. This solution is used for a classical chatter analysis according to the equations: 1–3.

The algorithm assumes that bifurcations can exist in the structure, so there could be more than one stable solution for some loading conditions, and all these unique solutions must be analysed. In the final step, we synthesise all these solutions, and all possible solutions are compounded into a general lobe diagram.

5.3 Dynamic Response of Simulated Modal Hammer Impulse and Comparison of SLOP Lobe Diagram With Time-domain Simulation

As we showed in the motivation part, some irregularities could occur during the modal hammer measurement - different hit peaks cause changes in the system response. Structural non-linearities could cause this behaviour. Therefore, the time-domain simulation of the modal hammer measurement was applied to the presented nonlinear structure to verify this behaviour. The input signals that follow the force signals in Fig. 2 were applied to the analysed structure. The resulting deflection was then transformed by the Fast Fourier transform (FFT) to frequency domain dynamic compliance in Fig. 11. The results show that the system response depends on the modal hammer hit property, the maximal peak frequency, and the changes in shape. Hence, the model presented could represent the frequency shift and the change in the peak shape.

Figure 12 shows the results of time-domain simulation 3D graph of the maximal knife amplitude. The results resemble a steep cliff from the front edge of the instability (lobe

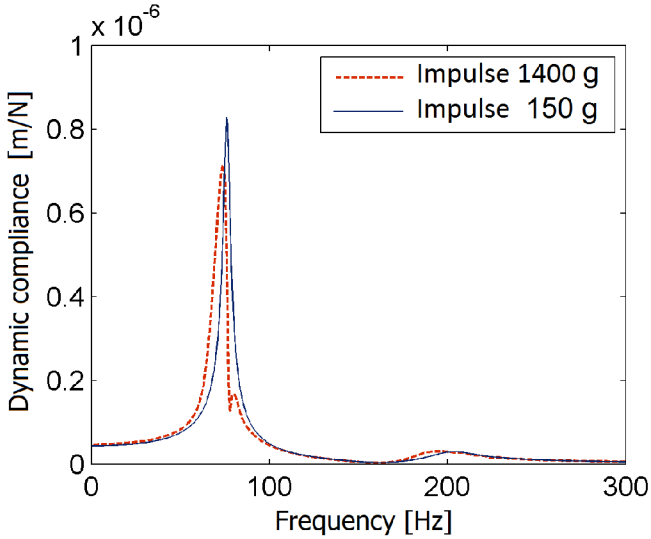

Figure 11: Simulated impact response

edge which is defined by the system's range from natural frequency to min real part range) and sloping down to the back edge of instability (lobe edge which is defined by the spectrum above min real part range). Below the 2 mm chip width, the highest amplitude

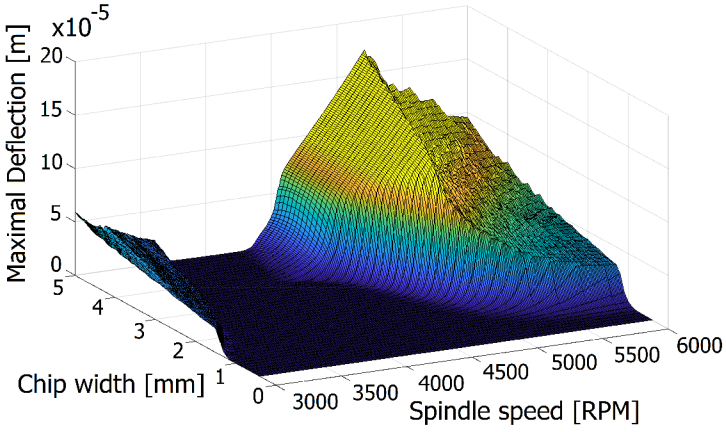

Figure 12: Time-domain simulation detection of maximal deflection depending on the chip width and spindle speed

ridge follows the edge of the stable system; above it bends towards lower speeds where at its minimum point it changes the trend, and with higher chip width it grows towards higher speeds.

The projection of the stable and unstable region and comparison with the SLOP results is in Fig. 13. The results of both SLOP and time-domain simulations show that even the system based on the Hertzian contact theory causes noticeable changes in the chatter stability. In both results, we can notice the front side's deformation approximately in the lobes, mainly in the area from 3 mm to 4 mm chip width where the stability drops to the lower spindle speed; above this area, the trend changes, and the lobe's edge is deformed following the higher speed. However, the SLOP solution provides a more conservative stability estimation. The backside of the lobe provides different results, wherein the

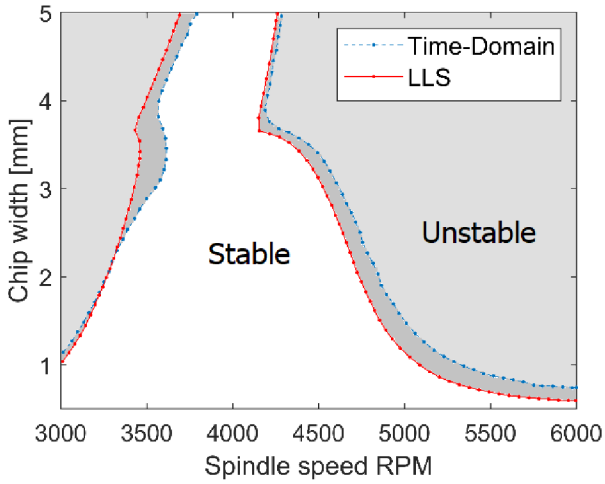

Figure 13: Time-domain simulation detection of maximal deflection depending on the chip width and spindle speed

results above 2.5 mm chip width time-domain simulation offer better results.

6 Nonlinear Analysis Using Substructuring Approach

To obtain an accurate prediction of the stiffness behaviour of the guideway, it is necessary to integrate an FEM model with the nonlinear model of the LBG. However, most FEM packages support nonlinear elements only without preload, and hence it is impossible to apply such models directly to the problem considered, in which the LBG is subject to a preload force before the machining process begins.

Accordingly, in the model proposed in this study, the guideway system is divided into a linear part and a nonlinear part, respectively. For the linear part, modal reduction is applied, which reduces the number of modes of the linear structure, whilst preserving the static behaviour of the defined contact nodes. Meanwhile, the nonlinear part is represented by eight nonlinear equations for each contact row. The nonlinear and linear are then joined in the Simulink environment using force - deflection relations in contact nodes.

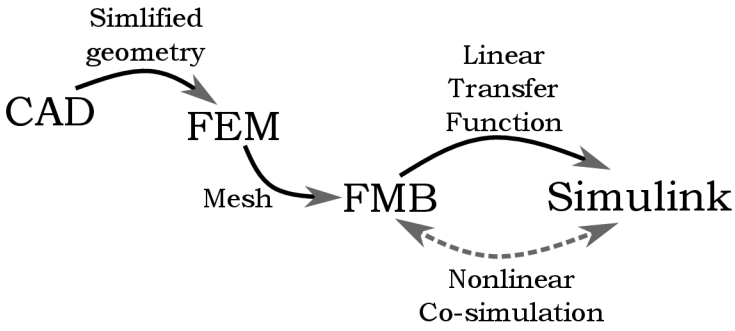

Figure 14: Scheme of Multi-body based nonlinear analysis

The basis of this nonlinear analysis is to substitute the mesh with linear behaviour by

reducing the transfer function, which interacts with nonlinear connections. The analysis is done in MSC Adams and MATLAB Simulink. The combination of these tools enables a wide range of analysis based on time-domain simulations.

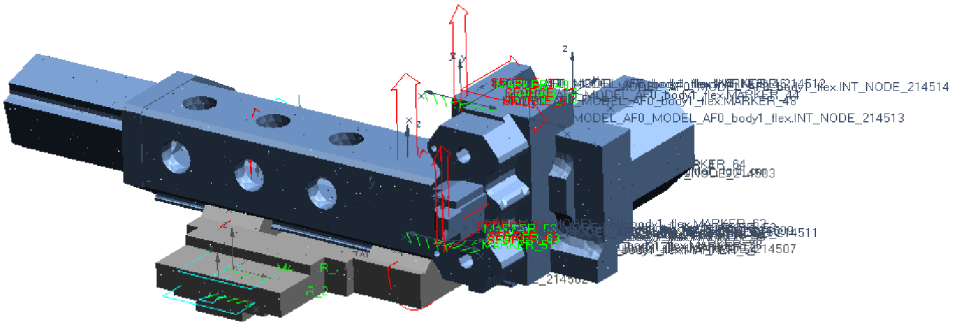

Figure 15: Adams model with boundary conditions and defined input and output connections

The first step is to the simplified CAD model, and the creation of reducing the modal structure of all linear parts of the structure at the same time is necessary to define the connection points on the mesh, which will be future inputs and outputs, in this case, force and deflection outputs, which will represent nonlinear connections and force input. A modal neutral file is used to import the reduced modal body into MSC Adams, a modal neutral file is used, which defines the body, the topology of the mesh, stiffness, mass, the moment of inertia of elements, and defines the connection points.

This file can then be opened in MSC Adams, where the connections between bodies and the surrounding space can be extended and defined as input and output. In the case of a linear structure, it is easy to add connections between bodies. Although MSC Adams and most FEM tools enable nonlinear spring connection definition, it also has limitations and is ineffective in linear ball bearing cases. Figure 15 shows the flexible model with defined force inputs and observed reaction points.

The possible way is to transfer this model to MATLAB Simulink, where the nonlinear connections could be easily represented. Simulink also enables the simulation of regenerative chatter during the cutting process. To transfer the model into Simulink, there are two possibilities of exporting from Adams a linear state-space representation of the model or exporting a nonlinear model, which works as a bridge between Adams and Simulink; however, it requires the cooperation of both programmes at the same time. During the model exporting, algebraic loops should be considered, which could happen due to the direct flow of the feedback loop into the state-space model. It is advantageous to use variables with higher orders of derivation, velocity, or acceleration, rather than position, to avoid this problem. If we consider that a linear behaviour can represent our model's main structure, it is better to export a simulated linear state space model without MSC Adams. This set of transfer functions usually has high-frequency compounds that interact with the numeric solver, leading to many problems, for instance, numeric instability or the requirement of minimal computational step size. The reduction of the model could be applied to suppress the high-frequency modes of the system to avoid these problems. Reduced values also increase the computation speed. Due to the modal reduction in previous steps, these responses are not valid and accurate; secondly, they are irrelevant for

cutting stability or nonlinear connection analysis. In Simulink, the reduced state-space model can be easily connected to the model of a linear ball guideway. This model could be used to simulate forced vibration, hammer impact, or stability during machining.

6.1 Reaction in linear ball guideway analysed by multibody based s on static load reaction analysis

The key advantage of this cosimulation model is that it enables the substitution of different types of analysis using the same model. Static load analysis represents a two-step load, where the first represents the gravity load and the second the cutting force. Due to the dynamic character of the model, it is necessary to simulate the model until the steady condition.

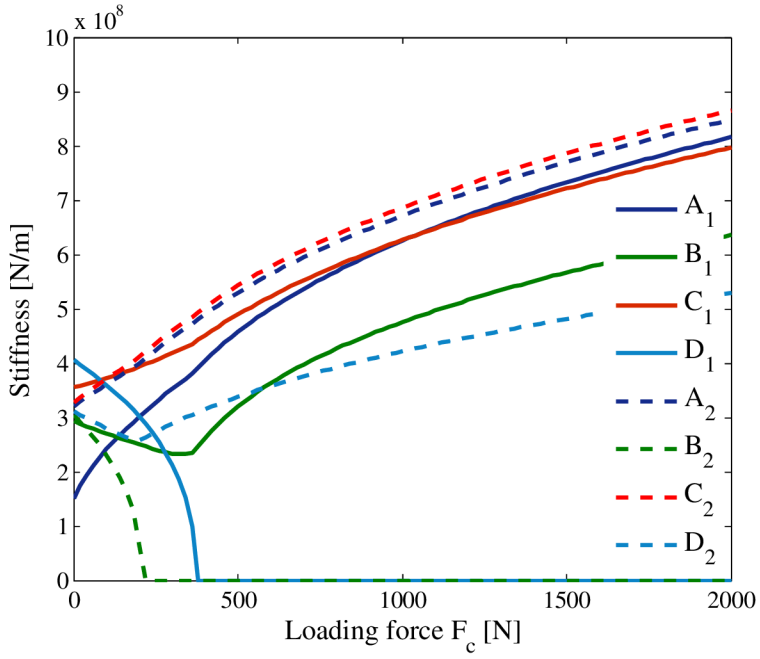

Figure 16: Variation of stiffness with loading force for individual ball rows in LBG structure.

The simulated static load follows the trends of the previous analysis with minor differences. Fig. 16 shows how the rows depend on the load of the knife during the grooving operation. The difference between this analysis and the results of the previous model is a significant change in the B_2 stiffness drop. The leading cause is the flexibility of the structure under the front bound (A_1-D_1) that limits the torque loading capacity. Due to this behaviour, the rear contact has a higher reaction force and a stiffness drop.

The analysis of stiffness behaviour in contact is essential for future dynamic research. The stiffness values could be used in the modal analysis to estimate linearised mode shapes. However, the most important role is to identify regions with a significant change of behaviour. In the presented case, the area is 200 – 500 N, where a slight change in the loading force significantly changes the dynamic behaviour of the system.

6.2 Frequency Responses and Impact Simulation

As shown in Fig. 17, the first two frequency modes of the guideway show a two-step drop in frequency as the loading force increases as a result of the structure's compliance below LBG.

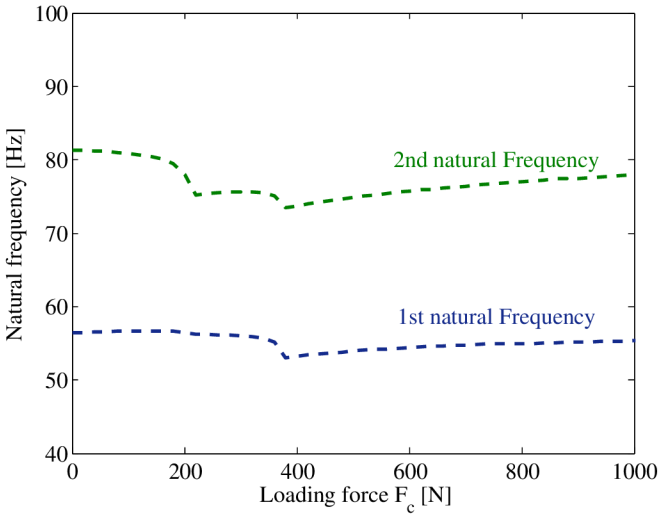

Figure 17: Dependence of first two natural frequencies of guideway on cutting force F_c.

The minimum frequency drop moves to the higher frequency to 73 Hz; this is caused by that the minimal stiffness of both LBG do not meet in the same load. The third frequency mode has a frequency of -160 Hz; however, it does not have a significant trend in load dependency; therefore, Fig. 17 shows only the first two modes.

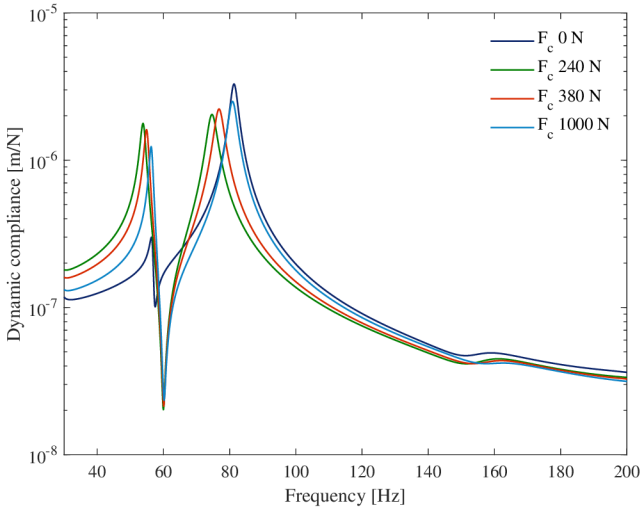

Figure 18: Dynamic compliance of tool tip under gravity force and combined gravity force and three cutting loads F_c.

The main benefits of the cosimulation model are the reliable prediction of dynamic compliance. The results of dynamic compliance substructuring are presented in Fig. 18.

The second mode decreases its compliance. Above the load of 380 N, the trends change and the first mode decreases and the second mode increases. Since static substructuring analysis considers the guideway structure to provide a more reliable load distribution, it will be used for the following prediction of vibrations.

7 Chatter Stability and Frequency Estimation Application of SLOP Algorithm

As mentioned above, chatter stability is an essential property of machine tools. However, it is difficult to predict the chatter behaviour of structures with nonlinear joint stiffness since the dynamic compliance of the overall system is load dependent. To solve this problem, the SLOP algorithm was proposed. Using the SLOP algorithm, it is possible to estimate the bode stability diagram for a nonlinear system. The following chapter presents an application of the SLOP algorithm to the cosimulation static model and estimates the response of the chatter frequency. This step enables future experimental validation.

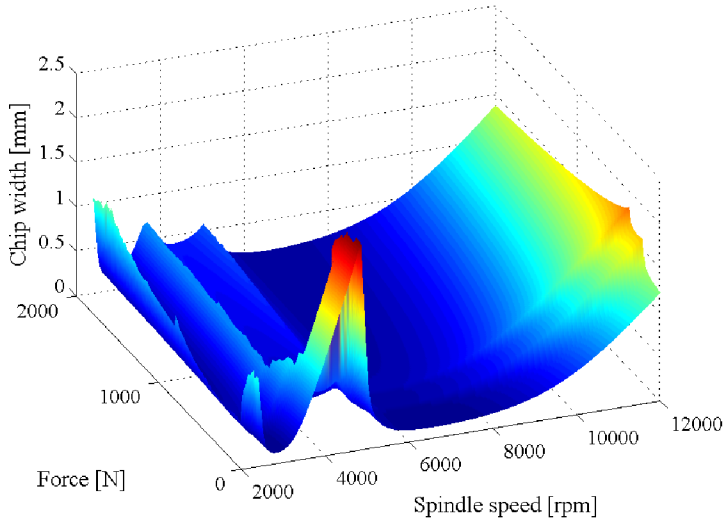

Figure 19: Estimated linearised chatter stability lobe diagram of LBG structure as function of static load.

Linearised systems are applied to equations 1-3; the solution of these equations gives the stability limits for the LBG under different cutting loads (see Fig. 19). In other words, for each static load that acts on the tool, there exists a particular linearised dynamic characteristic of the system and a unique stability diagram exists for the load of each static system. Figure 19 shows a significant discontinuity in stability in the minimum system of $F_c = 375$ N. However, a more minor discontinuity is also observed at $F_c = 218$ N, corresponding to the loss of contact at B_2.

The cross-sections of the surface in Fig. 19 represent the stability lobes for different cutting forces. Figure 20 shows four illustrative cross-sections corresponding to loads of 0, 200, 400, and 900 N, respectively. Note that the force of 0 N corresponds to the case where the structure is loaded only by gravity and is an important value, since the boundary thus corresponds to that obtained in impulse-hammer measurements when the structure is unloaded.

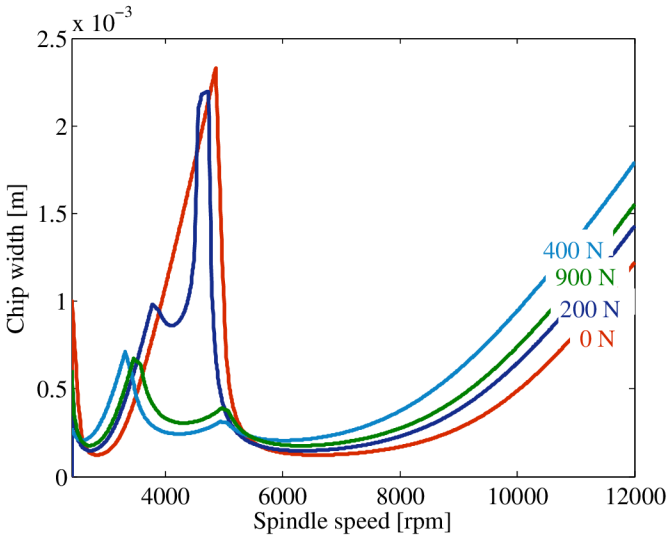

Figure 20: Illustrative stability lobe diagrams for structures linearised under different loads.

It is noted that in this condition, stability prediction based on impulse hammer measurement is likely to be highly unreliable for the higher load - with increasing load the stable area between the two lobes is filled with new instability, and the stable area for the unloaded system becomes highly unstable after loading. Paradoxically, the highest criterion of the unconditional stability band has a load in the case of minimum rigidity, and with the lower system compliance the lobe shifts to a lower spindle speed. As the load increases, the area between the two lobes decreases slightly, and the lobes move toward higher spindle speeds (as evidenced by the curves for 400 N and 900 N, respectively).

In the lathe machining process, the cutting load depends on the chip width, feed, etc. Therefore, for each loaf variable would be a different stability diagram which could be compiled using linearisation synthesis. The method used to create such a synthesis is described in Chapter 8. The algorithm arranges a stability diagram corresponding to the load. For illustration, stability diagrams were created for the feed of 0.1 and 0.05 mm/rev. However, it is possible to create any feed corresponding to a linearised range. The resulting diagram is then unique for every feed and cutting force.

Figure 21 shows an illustrative stability chatter diagram for feeds of 0.1 mm/rev and 0.05 mm/rev, respectively, given a specific cutting force of Ks = 2500 MPa. For a feed of 0.1 mm/rev, the lobe diagram has noticeable regions corresponding to a loss of contact at B_2 and D_1 are observed, resulting in notches in the range of 10000-12000 RPM at loads of 218 N and 375 N. The loss of contact in B_2 also affects the speed range of 3500-5000 RPM causes; with increasing load, the first mode becomes significant and reduces the stable area. For a lower feed of 0.05 mm/rev, the system behaves more like a linear system. In particular, the changes in the lobe diagram shape are less significant since due to lower load the more considerable changes shift to a higher chip width. In fact, the only change observed is a slight deformation of the connection of the lobes at 4500 RPM.

The stepped effect in the chatter stability diagram is given by the linearisation interval used for the nonlinear static analysis of the contacts in the bonds. Overall, the results presented in Fig. 21 show that the required fineness of linearisation increases with a reducing feed. Thus, when using consistent linearisation, this effect of linearisation intervals is more pronounced in the case of slower feeds. Part of the chatter stability prediction is

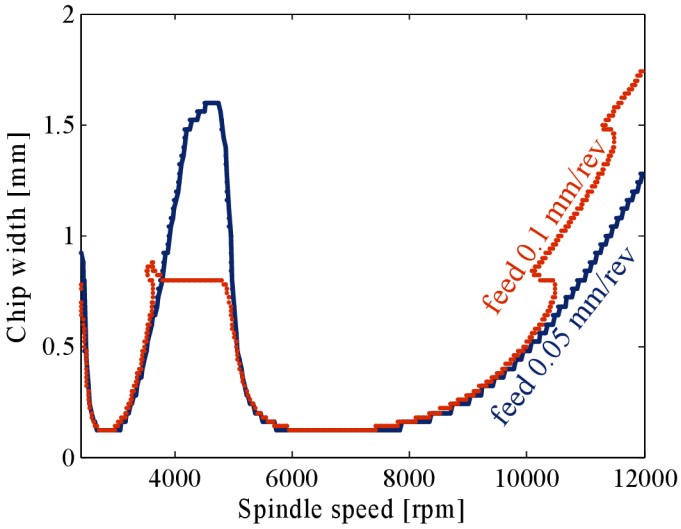

Figure 21: Stability chatter diagram compiled by synthesis of linearisation in operating points

also the frequency response analysis. Applying the linearised solution to Eq. (3) yields the predicted chatter frequency for specific cutting conditions. By monitoring the frequency response, the influence of both structural damping and process damping can be eliminated, thereby allowing the effects of stiffness nonlinearities to be reduced.

8 Experimental Setup

8.1 Comparison of Simulated Impulse with Impulse Hammer Measurements

The cosimulation model enables time-domain simulation. It is thus feasible to simulate the structure response for a particular impact and compare the results with the corresponding experimental observations and linearised solutions. In the present study, the simulation input was taken as the force signals acquired in real-world impulse hammer tests. The hammer impact points and sensor locations used in the experimental and simulation processes are shown in Fig. 22.

Figure 23 compares the experimental and simulation results for the dynamic compliance of the test structure under the effects of a 160 g impulse. It is noted that the measurement results correspond to the modelled values. In general, the results show that the second mode has the lowest dynamic stiffness in the x-direction. In addition, the simulation results for the third mode frequency are around 30 Hz higher than the measured data. The higher modes in comparison then approximately correspond in frequency position but differ in peak size.

The model assumes a constant damping parameter, and higher frequencies are thus attenuated compared to the experimental results. However, the stability of the considered system depends mainly on the frequency shifts which occur at low frequencies (i.e., the first two modes), and hence discrepancies between the measurement and model are insignificant. In addition, its significance is enhanced by the logarithmic scale of Fig. 23.

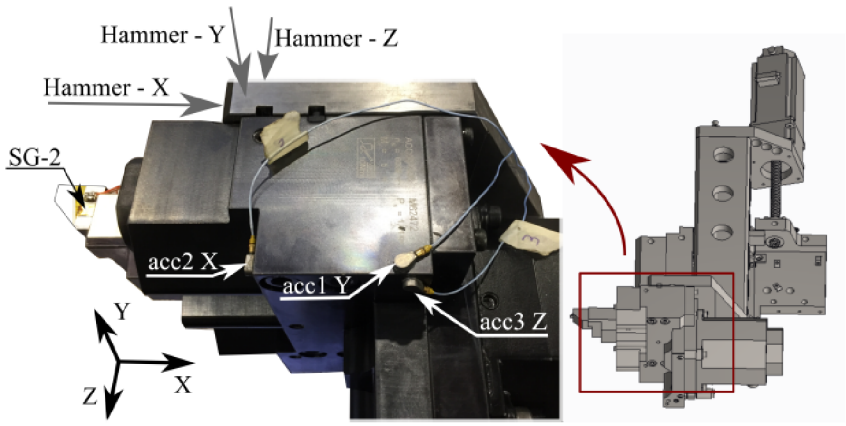

Figure 22: Positions of impact points and accelerometers in experimental and simulation processes.

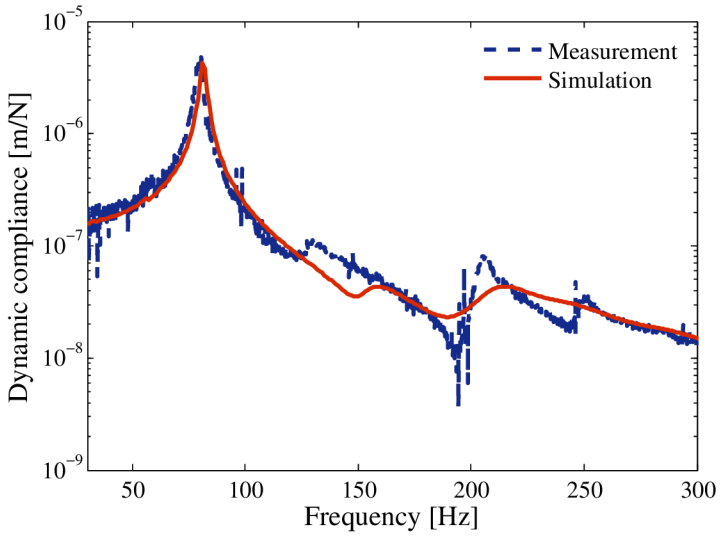

Figure 23: Comparison of simulated and measured dynamic compliance of test structure in x-axis direction given impulse force of 160 g

8.2 Experimental Machining Trials for Chatter Behaviour Verification

In practice, experimental verification of the chatter behaviour faces several key challenges, including the low stability of the system itself and the fact that there is no stable area between the lobes in the stability diagram at lower speeds, the area practically filled with harmonic lobes without any windows of higher chip width stability.

Due to the dimensions of the tested structure and the requirements for independent movement, the verification trials were performed on a large horizontal milling machine (TOS WHN 13 A), which allowed both the spindle function and table movement to change the chip width and ensure feed in the cut. The milling machine provided several advantages for the verification process, including most notably its large dimensions and sliding guide mounting, which allowed its dynamics to be isolated from those of the tested LBG system. However, the machine offered only a very limited choice of spindle speeds

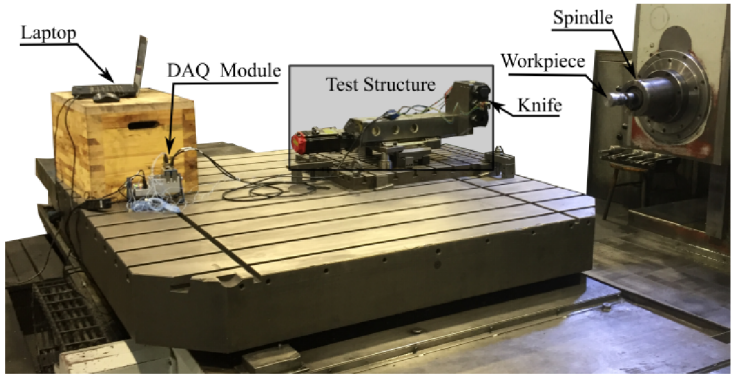

Figure 24: Photograph of experimental setup used to verify chatter behaviour of LBG.

for the cutting process (i.e., 430, 465, 600, and 765 RPM). Consequently, the acquisition of an experimental lobe diagram was almost impossible, and hence the only feasible option for evaluating the chatter behaviour of the guideway was to verify the frequency response under unstable machining conditions.

Figure 23 presents a photograph of the experimental setup. As shown, the guideway was mounted on a milling machine table. Strain gauges were attached to the tool holder to reconstruct the force load, and accelerometers were applied to the body of the system to measure vibration in different directions during the machining (Fig. 22). The signals generated by the strain gauges and accelerometers were collected by a DAQ module and interfaced to a PC for subsequent processing. The workpiece was a steel cylinder (C45) with a diameter of 70 mm, it was mounted on the spindle of the horizontal milling machine. In the machining trials, grooves were cut into the end face of the workpiece with a grooving width in the range of 1 to 4.5 mm with increments of 0.5 mm.

As the width was increased, the depth was gradually reduced from 3 mm to 1.4 mm in steps of 0.2 mm. For each machining condition (i.e., groove width and depth), two trials were performed in order to ensure the reliability of the measurement results. The signals acquired from the strain gauges and accelerometers were used to construct a corresponding power spectral density (PSD) diagram from which the frequency response of the system was then determined.

9 Results and Discussion

The PSD maps in Figs. 25 (a) (d) show the dependence of the response frequency of the experimental structure in the x-axis direction on the width of the chip at spindle speeds of 430, 465, 600, and 765 RPM, respectively. The most significant spectral changes are observed at a spindle speed of 765 RPM, for which a frequency component of 74 Hz, which is not predicted by linear theory, is detected at machining depths greater than 4 mm. (A similar phenomenon also occurred at the other spindle speeds; however, the signal strength was far weaker and is thus not easily seen in the corresponding PSDs. For spindle speeds of 430 RPM and 465 RPM the PSD changes in the area above 3 mm, multiple new spectra occur, and the original peaks are expanding. The least noticeable is the spectral change in PSD at 600 RPM where these changes in PSD are the weakest and when there are small changes for data above 4 mm. These changes can also be observed at higher harmonic frequencies.

The spectral changes observed in the PSDs can be attributed most feasibly to the

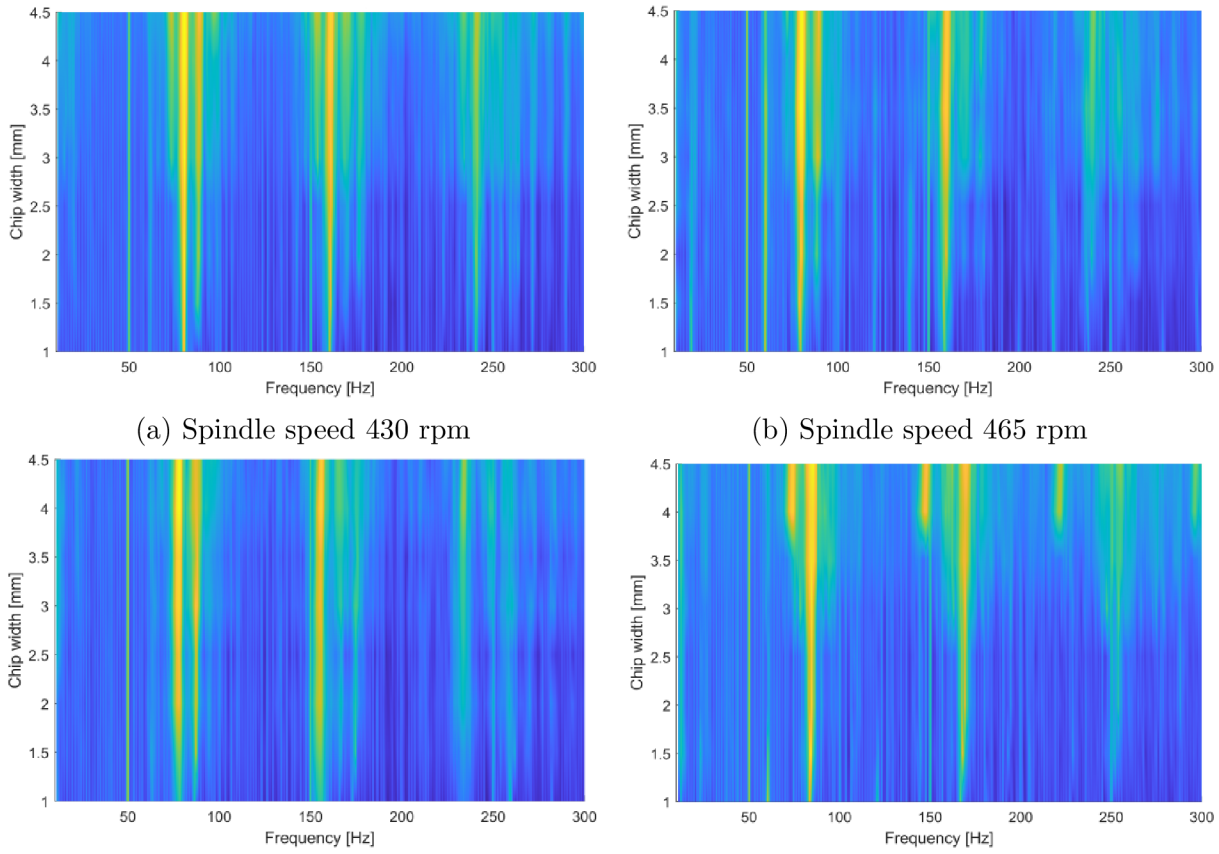

(a) Spindle speed 430 rpm

(b) Spindle speed 465 rpm

(c) Spindle speed 600 rpm

(d) Spindle speed 765 rpm

Figure 25: Experimental results obtained for frequency response of experimental structure in x-axis direction given different chip widths and spindle speeds (430, 465, 600, and 765 rpm).

nonlinearity of the system. The nonlinear model presented in Section 4.2 accurately depicts the behaviour of the system and the aforementioned spectra, whereas a simple linear approach cannot. Figures 26 (a) and (b) compare the chatter frequencies predicted by the nonlinear model and a linear model for chip widths of 1 mm and 4.5 mm, respectively. It will be recalled that the linear model does not consider the change in system stiffness caused by the load and represents the results obtained in impulse hammer measurements. For reference purposes, the estimated spectra are compared with the experimental data acquired by the strain gauges, which more accurately describe the self-excited frequency responses and eliminate the surrounding influences of random excitation. The size of the plotted points corresponds to the signal strength of the corresponding PSD and hence provides an indication of the measured instability. In other words, the points indicate the most dominant chatter frequencies.

It should be noted that the results correspond to unstable cutting conditions. Although the chatter has an impulse character, during its initialisation, the static component of the cutting force is dominant and the force oscillates around the value of the static force. Therefore, the static force component is expected to load the LBGs, resulting in initialising the corresponding chatter frequency. Consequently, the linearised estimates for frequency prediction are not as accurate as those for the machining process performed at the edge of stability, since, during unstable cutting, the tool passes through many different stiffness states.

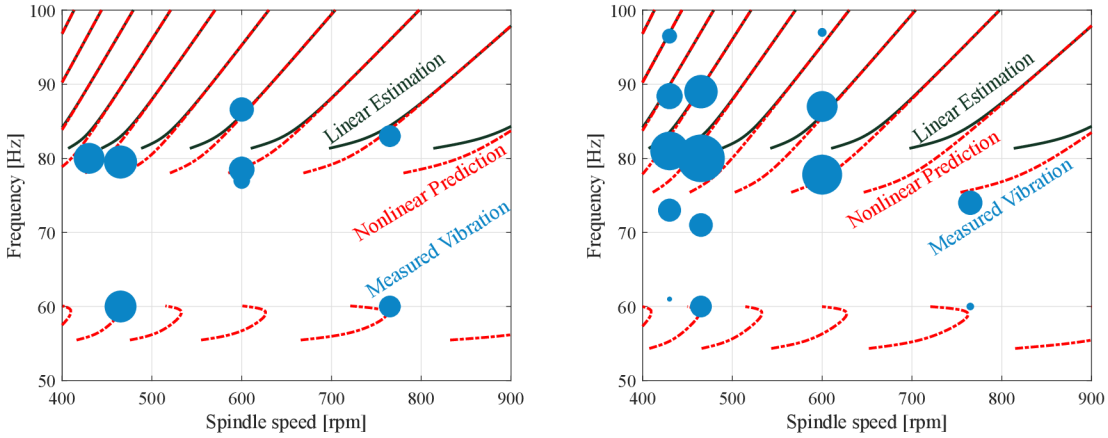

(a) Chip width 1 mm (b) Chip width 4.5 mm

Figure 26: Comparison of estimated frequencies of chatter vibration and scaled measured response obtained in experimental trials for chip widths of: (a) 1 mm and (b) 4.5 mm.

Nonetheless, despite this limitation, the estimates obtained using the cosimulation model are in good qualitative agreement with the measurements results for the self-excited vibrations. In most cases, the estimates deviate from the measured frequencies by no more than 2 Hz. However, more significant deviations are observed for the largest chip width of 4.5 mm and lower spindle speeds (430 465 RPM). For example, an estimation error of 5 Hz occurs at 465 RPM, while an error of 3 Hz occurs at 430 RPM. Notably, these findings confirm the nonlinear behaviour of the system since, according to linear theory and impulse hammer measurements, no vibration should occur in the spectrum band of 70 80 Hz.

Overall, the results confirm that the nonlinearity of the LBG structure must be taken into account especially when the external load causes preload loss. Furthermore, the measurements obtained by a modal hammer for such structures provide only limited information about the structure response. In future work, the linearisation method applied in the present study for stability estimation will be integrated with a process damping model to better describe the system response in the low-speed region. Furthermore, the estimation performance will be enhanced through the application of a stochastic approach to the dispersion of the specific cutting force and the definition of the probability band of the stability lobe diagram.

10 Proposed Methodology of Machine-Tool Design

Like many natural processes, a logistical function can also describe technical development. In many cases, it seems that the current types have reached the top and therefore that further efforts to improve will not lead to a better product, especially in terms of the layout of the machine structure. As was evident in the previous chapters, the influence of nonlinear bounds on the overall machine behaviour is underestimated during the machine's design and operation. Therefore, it is necessary to reconsider the methodology of structural design. The design should focus on the whole system and optimisation of partial structures considering the load flow in the structure, which leads to an iterative

process, where the first part focusses on the appropriate distribution of links. The creation of dynamic substructures decomposes the overall assembly into substructures, so it is possible to solve separate tasks in parallel; then it is necessary to verify the overall machine behaviour.

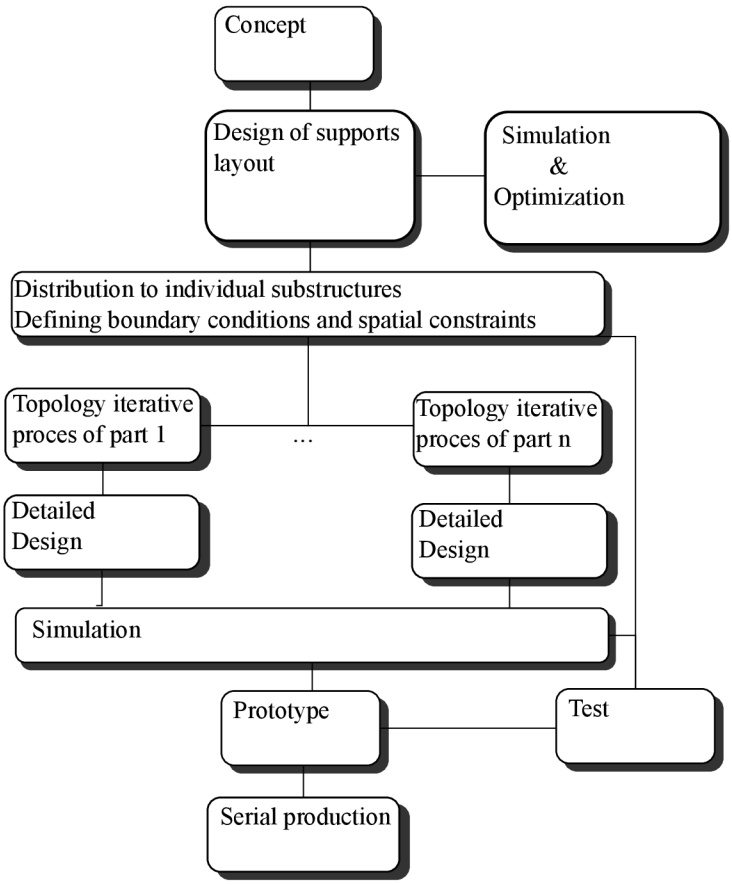

Figure 27: Scheme of development of new machine tools

It is often very difficult to apply loads from the cutting process, as they are very variable and depend on the type of technology, and even different batches of the same material can fundamentally change the behaviour of the cutting process. Therefore, it is necessary to approach the problem stochastically and not just choose deterministic conditions. Here, it is necessary to emphasise the effect of nonlinearities when even a small change in conditions results in a significant deviation of the change in result; as shown in the example presented, the load was able to reduce the natural frequencies of the system by ten percent and thus seemingly reduce system's stiffness 100 times. Knowledge of the behaviour of nonlinear bonds enables the improvement of the machine tool structure. For instance, the property of a linear ball guideway enables the use of both hardening and softening regions with the right design. Based on these assumptions, we can propose a development methodology. The scheme of the proposed methodology is shown in Fig. 27. Each machine design should begin by defining a basic machine concept and analysis of the expected load. In the first step, that is necessary to define the layout of the bonds between each piece of the structure. Optimizing layout and number and position is crucial for the whole structure-property.

In the first step, it is necessary to define the layout of the bonds between each piece of the structure. Optimising layout and number and position is crucial for the whole

structure-property. In this, a very vague first draught of the structure is necessary to estimate the load of each bond and optimise the layout using knowledge of the nonlinear behaviour of the bonds. The next step is to use substructuring and split the whole machine into single structures, which could be optimised independently, knowing the load in the connections between them. All the parts should be of more detailed design. Furthermore, the structure should be simulated again as a whole, and if the load distribution changes significantly, the process should return to the point of individual substructures and re-optimise them based on new knowledge. As soon as the input and output simulations differ minimally, it is possible to proceed to the production of a prototype. The prototype test verifies the behaviour of the machine tool behaviour and verifies the simulation model. If the prototype test satisfies the entering requirements, then serial production could start. However, if the requirements are not satisfied, then it is necessary to analyse the problem, namely redesigning the structure. The test data are also valuable for the verification of the simulation model and for its improvement.

11 Summary of Work Benefits

This work deals with the case of nonlinear behaviour due to nonlinear stiffness, the nonlinearities are commonly underestimated in machine design and regularly presented as unsolvable problems which over complicated the analysis and does not provide enough additional benefits to deal with them.

This work not only proves the importance of considering nonlinearities that can have a crucial effect on machine tool performance but also provides the effective way to deal with these cases. As the experimental data prove, the method enables providing more valid information than the simple linearisation in the unloaded stage, which is usually the only method used for evaluating the behaviour of the machine tool. This work also highlights that linear ball guideway deformation and stiffness cannot be considered as directionally independent and gravity must be considered as the important parameter influencing the system dynamic behaviour.

The better understanding of the nonlinear behaviour of the components and proper analysis improve the prediction of dynamic behaviour and, therefore, enable better machine tool design. Following the provided methodology, better chatter stability should be achieved. Better knowledge of machine tool dynamics enables better productivity using a larger area of stability.

The scientific benefits of this work are:

- Time domain cosimulation of nonlinear stiffnes model with modal reduced submodels,
- Proposal of an effective method for estimation stability lobe diagram based on synthesis of local linearisation – SLOP algorithm,
- Concept of machine tool design methodology using nonlinear bond analysis and substrucuring optimisation.

The application benefits of this work are:

- The presented methods enables design bounds layouts design and analyze force distribution in the structure in early stages of machine tool development,
- Improvement of machine tool chatter stability simulation and optimisation of machining process.

12 Conclusion

Machine tool analysis without considering nonlinearities could lead to wrong chatter stability assumptions. Therefore, nonlinear operation of a real machine cannot simply be estimated and analysed by the linear system. Neglecting nonlinearities could lead to an incorrect estimation of vibration stability. It may seem clear that linear analysis cannot simply represent nonlinear systems; still, nonlinear analysis is rarely used for machine tool analysis and estimation of chatter stability prediction. Primarily for its simplicity, linear chatter estimation represents most of all analyses, regardless of the nonlinearity of the contact bonds.

This work presents an example of a machine tool with nonlinear stiffness that has a critical influence on its chatter behaviour. Step-by-step analysis uncovers the cause of this behaviour of nonlinearities and describes the phenomenon of linear ball guideways in the early stages; the analysis focusses on the time-domain simulation of the machining process, which in later stages become too computationally demanding. To effectively predict the system chatter stability lobe, the linearisation method was presented. This method was compared with the simulation of the simplified structures; because of promising results, the method was applied to the experimental structure. Two methods of nonlinear static analysis were applied in the experimental structure, the first was the simplified analysis based on contact reactions, and the second used dynamic sub-strusturing and cosimulation to estimate contact load in the nonlinear bounds. The first method represents the basic analysis, which could be used as the first draught of the behaviour; however, more precise results were obtained by the cosimulation method. Using the linearisation scheme and cosimulation mode, the chatter frequencies and the stability lobe diagram were estimated. Experimental machining trials were compared with prediction and show good match; the biggest deviation was within the 3 Hz range.

The ‘mystery’ of the shifted chatter frequency was revealed. The nonlinearity plays a key role in machine tool systems and could cause a large change of dynamic behaviour. Therefore, this phenomenon is necessary during the design and operation. The experimental data prove that propose analysis could provide valid chatter prediction. Information about the behaviour of the boundaries should be considered during the first draught of the linear ball guideway layout to prevent the with minimal stiffness from operating machine in the limits. For this, the simplified static analysis provides enough information. The more complex cosimulation is more suitable for analysing structure during more advanced development stages and for analysing operating condition of machine tools. The analysis scheme could be applied to other types of nonlinear bounds which are crucial components defining the main machine tool property. Due to the non-intuitive character of the non-linear bound, ‘weird’ situations could occur where lower number of linear ball guideways could provide a better dynamic property. Therefore, the layout considering bounds nonlinearity provides a better design of machine tools.

References

[1] J. Tlustý, *Manufacturing Process and Equipment*. Upper Saddle River: Prentice Hall, 1. ed., 2000.

[2] B. Gegg, C. Suh, and A. Luo, *Machine Tool Vibrations and Cutting Dynamics*. SpringerLink : Bücher, Springer New York, 2011.

[3] S. Jiang, S. Yan, Y. Liu, C. Duan, J. Xu, and Y. Sun, "Analytical prediction of chatter stability in turning of low-stiffness pure iron parts by nosed tool," *The International Journal of Advanced Manufacturing Technology*, Nov 2018.

[4] Y. Altintas, "Modeling approaches and software for predicting the performance of milling operations at mal-ubc," *Machining Science and Technology - MACH SCI TECHNOL*, vol. 4, pp. 445–478, 11 2000.

[5] Y. Ayed, C. Robert, G. Germain, and A. Ammar, "Orthogonal micro-cutting modeling of the ti17 titanium alloy using the crystal plasticity theory," *Finite Elements in Analysis and Design*, vol. 137, pp. 43 – 55, 2017.

[6] E. Turkes, S. Orak, S. Neşeli, M. Sahin, and S. Selvi, "Modelling of dynamic cutting force coefficients and chatter stability dependent on shear angle oscillation," *The International Journal of Advanced Manufacturing Technology*, vol. 91, pp. 679–686, Jul 2017.

[7] Z. Fu, X. Zhang, X. Wang, and W. Yang, "Analytical modeling of chatter vibration in orthogonal cutting using a predictive force model," *International Journal of Mechanical Sciences*, vol. 88, pp. 145 – 153, 2014.

[8] M. Eynian, H. Onozuka, and Y. Altintas, "Chatter in turning with process damping," *Proceedings of the 22nd Annual ASPE Meeting, ASPE 2007*, 01 2007.

[9] Y. Altintas, M. Eynian, and H. Onozuka, "Identification of dynamic cutting force coefficients and chatter stability with process damping," *CIRP Annals*, vol. 57, no. 1, pp. 371 – 374, 2008.

[10] M. A. Rubeo and T. L. Schmitz, "Global stability predictions for flexible workpiece milling using time domain simulation," *Journal of Manufacturing Systems*, vol. 40, pp. 8 – 14, 2016. SI:Challenges in Smart Manufacturing.

[11] W. Sun, X. Kong, and B. Wang, "Precise finite element modeling and analysis of dynamics of linear rolling guideway on supporting direction," *Journal of Vibroengineering*, vol. 15, no. 3, pp. 1330–1340, 2013.

[12] W. Sun, X. Kong, B. Wang, and X. Li, "Statics modeling and analysis of linear rolling guideway considering rolling balls contact," *Proceedings of the Institution of Mechanical Engineers, Part C: Journal of Mechanical Engineering Science*, vol. 229, no. 1, pp. 168–179, 2015.

[13] X. Kong, W. Sun, B. Wang, and B. Wen, "Dynamic and stability analysis of the linear guide with time-varying, piecewise-nonlinear stiffness by multi-term incremental harmonic balance method," *Journal of Sound and Vibration*, vol. 346, pp. 265 – 283, 2015.

CURRICULUM VITAE

Petr Hadraba

Education

- **2017 - 2023 Doctoral** – BUT, Faculty of Mechanical Engineering, Machines and Equipment - Design and Process Engineering
- **2015 - 2017 Master** –BUT, Faculty of Mechanical Engineering, Applied Sciences in Engineering - Mechatronics
- **2012 - 2015 Bachelor** – BUT, Faculty of Mechanical Engineering, Engineering, Fundamentals of Mechanical Engineering
- **2008 - 2012 High School/Senior High School** Gymnázium Kojetín

Internship

- **2019 October–December** National Cheng Kung University, Taiwan, Prof. Wang's Chatter research lab
- **2023 February–March** National Applied Research Laboratories, National Center for High-Performance Computing, Taiwan Physical Informed Neuro Networks in dynamic modelling

Experience

- **2014 - 2017 Tajmac-ZPS MORI-SAY Division** 3D modeling and creation of drawing documentation
- **2017 - 2022 Tajmac-ZPS MORI-SAY Division** Computational and experimental analysis of machine tools
- **2020 Institute of Solid Mechanics, Mechatronics and Biomechanics FME, BUT** Railway track stand design
- **2022 Benecykl s.r.o.** Development of a sensory stroller for the disabled

Language skills

Czech – mother tongue, **English** – Upper-Intermediate, **Chinese** – Elementary

Other Skills

MATLAB Simulink and Python – Data processing and numerical simulation, **MSC Adams**– Multi body simulation, **Ansys** – Modal and harmonic analysis, **Inventor, PTC Creo, and Solidworks** – Parametric modelling and technical drawing, **TensorFlow** Basic neuro-network modelling **Driving license**

Abstract

Nonlinear stiffness affects the dynamics of modern machine tools. An important parameter of machine tool productivity is self-excited vibration, which limits the performance of the machine tool. This work was motivated by an industrial case where the behavior of a machine tool cannot be predicted by traditional methods and the machine exhibits a significant change in dynamic behavior. This work presents a step-by-step analysis that was focused on the simulation of self-excited vibrations and the effect of nonlinear stiffness on the resulting vibration stability. As the complexity of the model increases, a linearization approach has been introduced that allows faster analysis of machining stability. For better mapping and creation of a stability lobe diagram for a nonlinear structure, an algorithm for the synthesis of linearized solutions at the working point is presented. The linearization approach was combined with nonlinear static simulation considering the nonlinear behavior model of the linear ball guide and used to predict the vibration behavior. The nonlinear static model uses a dynamic cosimulation and substructuring method to incorporate the effects of structural deformation into the analysis. The experimental machining test made it possible to compare the analysis results and demonstrated good agreement with the maximum frequency deviations in the 3 Hz band.

Abstrakt

Nelineární tuhost ovlivňuje dynamiku moderních obráběcícho strojů. Důležitým parametrem produktivity obráběcího stroje jsou samobuzené vibrace, které omezuje výkon obráběcího stroje. Tato práce byla motivována průmyslovým případem, kdy chování obráběcího stroje nelze předvídat tradičními metodami a stroj vykazuje významnou změnou dynamického chování. Tato práce krok za krokem představuje analýzu, která byla zaměřena na simulaci samobuzených vibrací a vlivu nelineární tuhosti na výslednou stabilitu chvění. Se zvyšující se složitostí modelu byl představen linearizační přístup, který umožňuje rychlejší analýzu stability obrábění. Pro lepší mapování a tvorbu stabilitního lobe diagramu pro nelineární strukturu je uveden algoritmus syntézy linearizovaných řešení v pracovním bodě. Linearizační přístup byl kombinován s nelineární statickou simulací s ohledem na model nelineárního chování lineárního kuličkového vedení a použit pro predikci chování chvění. Nelineární statický model využívá metodu dynamické kosimulace a substrukturování, aby do analýzy začlenil účinky strukturální deformace. Experimentální zkouška obrábění umožnila porovnat výsledky analýzy a prokázala dobrou shodu s maximálními frekvenčními odchylkami v pásmu 3 Hz.